2018

Impact of High-Intensity Ultrasound on Strength of Surgical Mesh when Treating Biofilm Infections

Timothy Bigelow
Iowa State University, bigelow@iastate.edu

Clayton L. Thomas
Iowa State University, clthomas@iastate.edu

Huaiqing Wu
Iowa State University, isuhwu@iastate.edu

Kamal M.F. Itani
Boston University and Harvard Medical School

Impact of High-Intensity Ultrasound on Strength of Surgical Mesh when Treating Biofilm Infections

Abstract
The use of cavitation-based ultrasound histotripsy to treat infections on surgical mesh has shown great potential. However, any impact of the therapy on the mesh must be assessed before the therapy can be applied in the clinic. The goal of this study was to determine if the cavitation-based therapy would reduce the strength of the mesh thus compromising the functionality of the mesh. First, S. aureus biofilms were grown on surgical mesh samples and exposed to high-intensity ultrasound pulses. For each exposure, the effectiveness of the therapy was confirmed by counting the number of colony forming units (CFUs) on the mesh. Most of the exposed meshes had no CFUs with an average reduction of 5.4-log10 relative to the sham exposures. To quantify the impact of the exposure on mesh strength, the force required to tear the mesh and the maximum mesh expansion before damage were quantified for control, sham, and exposed mesh samples. There was no statistical difference between the exposed and sham/control mesh samples in terms of ultimate tensile strength and corresponding mesh expansion. The only statistical difference was with respect to mesh orientation relative to the applied load. The tensile strength increased by 1.36 N while the expansion was reduced by 1.33 mm between the different mesh orientations.

Keywords
Ultrasound Therapy, Histotripsy, Biofilm Infection

Disciplines
Biology and Biomimetic Materials | Biomechanical Engineering | Biomedical

Comments
This is a manuscript of an article published as Bigelow, T. A., C. L. Thomas, H. Wu, and K. M.F. Itani. "Impact of High-Intensity Ultrasound on Strength of Surgical Mesh when Treating Biofilm Infections." *IEEE transactions on Ultrasonics, Ferroelectrics, and Frequency Control* (2018). DOI: 10.1109/TUFFC.2018.2881358. Posted with permission.

Impact of High-Intensity Ultrasound on Strength of Surgical Mesh when Treating Biofilm Infections

Timothy A. Bigelow, *Member, IEEE,* Clayton L. Thomas, Huaiqing Wu, and Kamal MF. Itani

***Abstract*— The use of cavitation-based ultrasound histotripsy to treat infections on surgical mesh has shown great potential. However, any impact of the therapy on the mesh must be assessed before the therapy can be applied in the clinic. The goal of this study was to determine if the cavitation-based therapy would reduce the strength of the mesh thus compromising the functionality of the mesh. First, *S. aureus* biofilms were grown on surgical mesh samples and exposed to high-intensity ultrasound pulses. For each exposure, the effectiveness of the therapy was confirmed by counting the number of colony forming units (CFUs) on the mesh. Most of the exposed meshes had no CFUs with an average reduction of 5.4-log$_{10}$ relative to the sham exposures. To quantify the impact of the exposure on mesh strength, the force required to tear the mesh and the maximum mesh expansion before damage were quantified for control, sham, and exposed mesh samples. There was no statistical difference between the exposed and sham/control mesh samples in terms of ultimate tensile strength and corresponding mesh expansion. The only statistical difference was with respect to mesh orientation relative to the applied load. The tensile strength increased by 1.36 N while the expansion was reduced by 1.33 mm between the different mesh orientations.**

***Index Terms*—Ultrasound Therapy, Histotripsy, Biofilm Infection**

I. Introduction

NUMEROUS new implantable medical devices continue to be developed with significant potential to revolutionize medical care. However, any time a new device is implanted, there is the risk of infections on the device. While proper surgical techniques can greatly reduce the risk of infection, surgical site infections (SSIs) still occur in alarming numbers. While some of these infections can be effectively treated by antibiotics, the implant can serve as a prime location for a bacteria biofilm. Bacteria biofilms are local communities of bacteria encased in a protective extracellular polymeric substance that are highly resistant to antibiotics [1]. Bacteria in the biofilm are also protected from antibodies [2, 3] and phagocytes [4, 5]. When bacteria biofilms are attached to an implant, the only treatment option is often the complete removal and replacement of the implant. Otherwise, the implant will continue to serve as a source of infection and may even lead to the development of antibiotic-resistant strains [6].

High-intensity focused ultrasound has already shown potential for non-invasively treating bacteria biofilms by using cavitation to disrupt the structure of the biofilm. Once the biofilm has been destroyed, any surviving planktonic bacteria will be susceptible to traditional antibiotic treatment. Prior studies successfully destroyed *Escherichia coli* (*E. coli*), *Pseudomonas aeruginosa* (*P. aeruginosa*), and *Staphylococcus aureus* (*S. aureus*) biofilms [7-10].

E. coli was selected as the first biofilm for test due to its prevalence in catheter-related infections [11]. For the *E. coli* experiments, the biofilms were grown on glass slides and exposed to pulses at different pressure levels using a 1.1 MHz spherically focused source [7]. The study found a threshold of 10 to 12 MPa for the rarefactional pressure for biofilm destruction with a typical reduction of 4-log$_{10}$ colony forming units (CFUs). As a comparison, high-level disinfection is defined by the FDA as a reduction in CFUs by 6-log$_{10}$. However, this level of bacteria destruction is difficult to achieve even *ex vivo*. For example, a basic cleaning of endoscopes typically only yields a 4-log$_{10}$ reduction in CFUs with additional soaking in high-level disinfectant for ~20 minutes needed to achieve a 6-log$_{10}$ reduction [12, 13].

P. aeruginosa was selected for the second study due to its general resistance to antibiotic treatment, and for its major contribution to nosocomial infections [8]. *P. aeruginosa* had also proven resilient to a non-cavitation based ultrasound treatment that attempted to use very long ultrasound exposures to enhance antibiotic diffusion into the biofilm [14]. For this experiment, the biofilms were grown on Pyrolytic graphite plates. The biofilms were then either exposed to a sham exposure or a series of 13 MPa tone bursts. The experiment varied the exposure duration at each location from 5 to 30 seconds and the period between the tone bursts from 1 to 12 ms.

Manuscript received September 20, 2018; accepted November 12, 2018. This research was supported by National Institutes of Health (NIH) grant number R21EB020722.

T. A. Bigelow is with the Center for Nondestructive Evaluation, Iowa State University, Ames, IA 50011 (e-mail: bigelow@iastate.edu).

C. L. Thomas is with the Center for Nondestructive Evaluation, Iowa State University, Ames, IA 50011 (e-mail: clthomas@iastate.edu).

H. Wu is with the Department of Statistics, Iowa State University, Ames, IA 50011 (e-mail: isuhwu@iastate.edu).

K. MF. Itani is with the VA Boston Healthcare System, Boston University and Harvard Medical School, West Roxbury, MA 02132 (e-mail: Kamal.Itani@va.gov).

The percent of live and dead bacteria on the plate was then determined by an epifluorescence microscopy image of the surface.

More recently, the studies have focused on treating *S. aureus* biofilms on surgical mesh samples [9, 10] due to the prevalence of *S. aureus* infections following hernia repair [15-17]. Infections on surgical mesh are one of the most significant complications and require mesh removal ~70% of the time with a significant risk of hernia reoccurrence following mesh removal [15-19]. The studies varied the tone burst duration as well as the step-size/scan speed utilized to expose the mesh. The reduction in CFUs relative to the sham exposures varied from 2.6-$\log_{10}$ to 4.3-$\log_{10}$ depending on the exposure conditions. These studies also quantified the level of collateral damage to healthy tissue in the vicinity of the mesh as a function of tone-burst duration.

In addition to damaging the bacteria biofilm, cavitation can also potentially damage the implant. Inertial cavitation near boundaries has an increased potential for damage due to the formation of microjets [20-22]. Microjets form due to the asymmetric collapse of the bubbles and can be used to erode metals [23-25]. However, the microbubble needs to be fairly close to the boundary (~ maximum bubble radius during bubble expansion) before a significant microjet can form. A material's resistance to microjet damage can be quantified to some extent by the indentation fracture toughness [26]. However, multiple factors play a role including surface roughness and the acoustic impedance of the material [27]. Therefore, it is often best to compare the materials experimentally.

The goal of this study was to determine if the cavitation activity in the vicinity of the mesh responsible for the biofilm destruction was negatively impacting the strength of the mesh. Since the purpose of the surgical mesh is to provide structural support during healing, compromising the strength of the mesh could result in hernia re-occurrence. Therefore, for this study, we used slightly longer exposures than our previous studies and measured the force required to tear the mesh for control, sham, and exposed mesh samples. We also measured the maximum change in dimension prior to mesh damage during tensile testing of the mesh.

II. Methods

A. Ultrasound Exposure Conditions

For the ultrasound exposures, 10 mm x 10 mm Polypropylene mesh samples (PPKM301, Surgical Mesh Division, Textile Development Associates Inc., Brookfield, CT) were inserted into Aquaflex Ultrasound Gel Pad Standoffs (Parker Laboratories Inc., Fairfield, NJ) as was done in our prior studies [9, 10]. The gel pads serve as easily reproducible sterile tissue mimics as they have approximately the same elastic modulus, ~53 kPa, as abdominal muscle [28-30]. The level of damage to soft tissue is directly related to the elastic modulus and therefore is the most important parameter when identifying an appropriate tissue mimic in histotripsy experiments [31-36]. The Young's modulus for polypropylene (material used for mesh fibers) is on the order of 1.1 to 1.7 GPa. However, prior studies showed that the damage that was dependent on the modulus was linked to the expansion of the bubble cloud in the material [34]. Therefore, the modulus is valid for assessing the risk of damage to the soft tissue but not to the implant.

After insertion, the gel pad with the mesh was placed inside an aluminum holder inside a water tank. The focus of the ultrasound transducer was then aligned on the mesh sample using a low-power signal from a pulser-receiver (Panametrics 5900, Olympus Corporation, Tokyo, Japan) as was done previously [9, 10]. The mesh samples were then exposed to either a sham exposure or a series of high-intensity ultrasound pulses.

For the exposures, the ultrasound transducer was continuously scanned in the horizontal direction while stepped in the vertical direction to sweep the focus of the transducer over the entire plane of the mesh similar to our earlier studies [10]. For this study, the step size was 400 μm (0.3 beam widths) and the scan speed was 0.3 mm/sec (0.23 beam widths/sec) where the –3dB beam width (BW) of the transducer was measured as 1.3 mm using a wire target. The focus was passed over the mesh 4 times for each exposure. For the sham exposures, the placement and scan of the mesh was the same, but the high-intensity ultrasound was left off during the scan.

The ultrasound transducer used in the study was a custom spherically focused transducer with an outer diameter of 82 mm and a focal length of 63.6 mm (H-184, Sonic Concepts Inc., Bothell, WA). The transducer also had a 39.9 mm hole to allow for the placement of an imaging probe for future *in vivo* experiments. For this study, the transducer was excited by a 3-cycle tone burst at 0.9 MHz with a 500 Hz pulse repetition frequency (PRF). The pulses were generated by a programmable function generator (Agilent 33220A, Santa Clara, CA) and then amplified by a high-power pulse amplifier (GA-2500A Gated RF Amplifier, Ritec Inc., Warwick, RI) before being sent to the transducer through a matching network as shown in Figure 1.

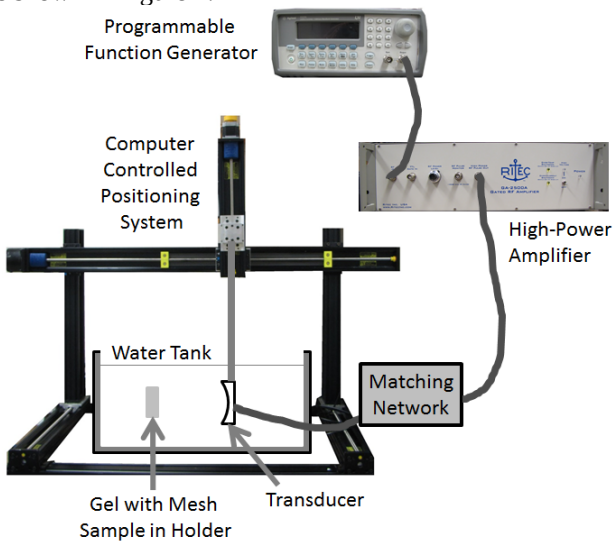

Fig. 1. The set-up utilized for the experiments when exposing the mesh samples to the high-intensity tone bursts.

Accurately measuring the pressure levels of high-intensity therapeutic ultrasound fields is challenging due to the production of inertial cavitation at the tip of the hydrophone potentially damaging the hydrophone. In addition, spatial averaging of the higher harmonics due to finite hydrophone size

can introduce errors in the field measurements, especially for the measurement of the peak-compressional pressure [37-39]. Therefore, a better approach is to measure the field away from the focus and then model the wave propagation at the focus using numerical methods [40-42]. In this work, the ultrasound waveforms were first measured on a plane perpendicular to the beam axis 15 mm in front of the focus using a capsule hydrophone (ONDA HGL-0200, Onda Corporation, Sunnyvale, CA). The waveforms were then input into K-Wave (http://www.k-wave.org/index.php) to find the fields in the focal region. K-Wave is a free MATLAB tool box that computes nonlinear propagation of ultrasound waves using a generalized form of the Westervelt equation [43].

In order to avoid running out of memory, the modelling was broken down into two regions. The first region extended from the measurement plane to 5 mm in front of the focus (10 mm depth) while the second region went from 5 mm in front of the focus to 5 mm past the focus (10 mm depth). The width and height of the regions as measured perpendicular to the beam axis were 36.4x36.4 mm for the first region and 14.2x14.2 mm for the second region. This corresponds to the beam radius for which the peak-peak pressure levels were within 20 dB of their maximum value. The mesh size and time step for the first region were 41.3 µm and 8.33 ns respectively, which corresponds to supporting 20 harmonics in k-wave. Likewise, the mesh size and time step for the second region were 20.6 µm and 4.17 ns respectively, corresponding to 40 harmonics in k-wave. The propagation medium in k-wave was water and had a sound speed of 1485 m/s, a density of 998 kg/m^3, and an attenuation of 0.0023 dB/(MHz^2-cm). The sound speed was based on a measurement of water temperature obtained during the hydrophone scan of the field.

While the method of combining measurement and modelling for calibrating highly nonlinear ultrasound fields is relatively well established, this was the first time our lab used this exact approach. Previously, we solved for the fields using a more limited Khokhlov-Zabolotskaya-Kuznetsov (KZK) based code that assumed continuous rather than pulsed excitation and was only valid for spherically focused transducers [8, 31, 44, 45]. Therefore, we needed to validate the accuracy of our new approach as has been done by other investigators [40-42]. Specifically, we measured the fields in the pre-focal plane at a lower excitation level for the transducer and compared the numerical results to the field measurements with the hydrophone placed at the focus. The fields were sufficiently low as to not induce cavitation and damage the hydrophone. The measured and modelled time domain waveforms for the lower excitation are shown in Figure 2.

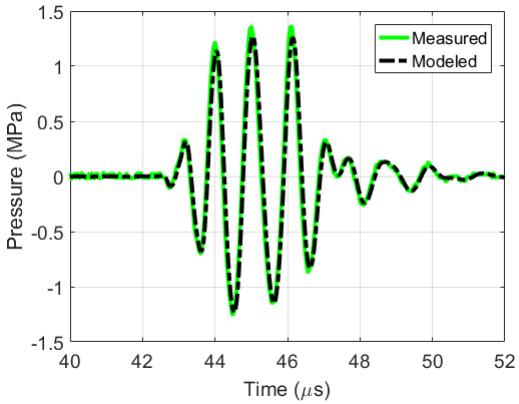

Fig. 2. Validation of combined measurement/modeling approach by comparing modeled waveforms with waveforms at the focus measured by a hydrophone at low transducer excitation.

There is agreement to within 1.6% for the peak rarefactional pressures and to within 6.5% for the peak compressional pressures. Therefore, our combined measurement and modelling approach is reasonably accurate when calibrating the ultrasound fields. The pressure waveform for the therapy excitation at the location of maximum rarefactional pressure is shown in Figure 3 while the maximum rarefactional and compressional pressures in the focal region were 9.2 MPa and 23.7 MPa respectively. These pressure values would be increased upon reflection from the mesh fibers.

B. Biofilm Preparation and Processing

Since the ultrasound exposure conditions were slightly different from our prior studies [9, 10], bacteria biofilms were grown on 16 of the mesh samples (8 exposed and 8 sham) to quantify the destruction of the biofilm at our new exposure level. To grow the biofilms, *Staphylococcus aureus subsp. Aureus (ATCC® 25923™)* was cultured on the mesh samples for 6 days at 37°C. On the first day, the mesh samples were placed in 20 ml of tryptic soy broth (TSB) that had been inoculated by 20 µl of stationary phase bacteria. On the subsequent days, the mesh was moved to a fresh 20 ml TSB solution each day so that the bacteria would have ample nutrients and thus continue to divide.

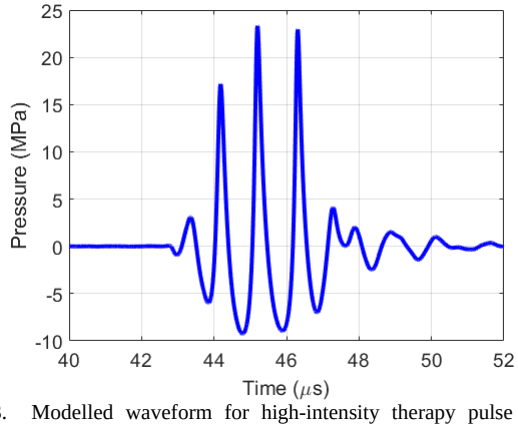

Fig. 3. Modelled waveform for high-intensity therapy pulse based on measurements made in the pre-focal plane.

This article has been accepted for publication in a future issue of this journal, but has not been fully edited. Content may change prior to final publication. Citation information: DOI 10.1109/TUFFC.2018.2881358, IEEE Transactions on Ultrasonics, Ferroelectrics, and Frequency Control

After the exposure or sham, the mesh was removed from the gel pad and briefly dipped in a tube of sterile phosphate-buffered saline (PBS) to remove any loose fragments. The mesh was then placed in a 1.5 ml micro-centrifuge tube with 0.5 ml of sterile PBS. The micro-centrifuge tube was then vortexed for one minute prior to being sonicated for two minutes in a Symphony Ultrasonic Cleaner (1.9 L, VWR, Radnor, PA). The tube was then vortexed for an additional minute, sonicated for two minutes, and then vortexed again for one minute. The sonication releases the bacteria from the mesh without killing them while the vortexing disperses the bacteria in the tube. After the last vortexing, 0.5 ml was removed from the tube and serially diluted in sterile PBS at dilutions of 10^{-1}, 10^{-2}, 10^{-3}, 10^{-4}, and 10^{-5}. Lastly, 100 µl of each dilution was then plated on tryptic soy agar plates and incubated overnight at 37°C.

After incubation, the number of CFUs on each plate was counted. The plates that had counts between 30 and 300 were then used to back calculate the total number of CFUs remaining on the mesh. Counts in this range are used as a well accepted rule of thumb in microbiology. Plates with fewer than 30 colonies may not give statistically reliable results, and plates with more than 300 colonies can be too crowded to allow the bacteria to form distinct colonies. If two different dilutions had counts in the 30 to 300 range, the back-calculated values were averaged. If no plates had counts in the desired range, the dilution whose count was closest to 300 was used. However, some of the exposures had no CFUs. After determining the number of CFUs, the counts were translated into a log number for comparison by calculating $\log_{10}(\text{count}+1)$ as was done in our earlier studies [9, 10].

C. Evaluation of Mesh Mechanical Properties

The potential impact of the ultrasound exposures on the mechanical properties of the mesh was assessed using a FTS-50X force test system (ABQ Industrial LP, The Woodlands, TX). The 10 mm x 10 mm mesh samples were placed with a 5 mm gap between the clamps as shown in Figure 4.

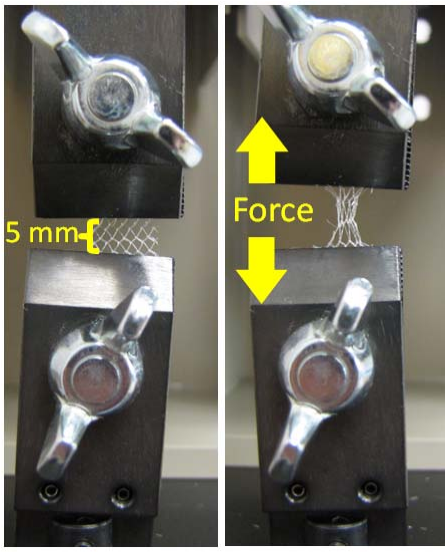

Fig. 4. Mesh samples in clamps of the force test system both before and after the force has been applied.

A force was then applied perpendicular to the mesh by turning a hand crank on the side of the test system that moved the clamps apart. One of the clamps was attached to a digital force gauge that provided the amount of force experience by the mesh. The ultimate tensile strength for each mesh sample was then given by the maximum force as read by the force meter. Digital calipers also measured the separation of the clamps at this force reading. Once the ultimate tensile strength was exceeded, additional turns by the hand crank did not increase the force and the individual mesh fibers began to break.

The weave of the mesh had two distinct orientations, A and B, as shown in Figure 5.

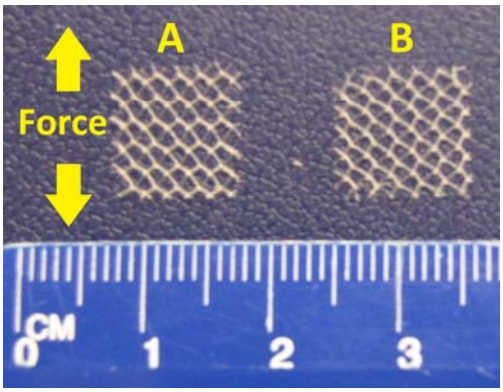

Fig. 5. The two different mesh orientations tested in the study.

The tensile strength experiment was repeated 15 times for each orientation for ultrasound exposed meshes, sham meshes, and control meshes. The sham meshes were placed inside the gel pad in the water tank for the same time as the exposed meshes while the control meshes were tested after being freshly cut from the mesh fabric. Therefore, a total of 90 meshes were tested in this portion of the study.

This article has been accepted for publication in a future issue of this journal, but has not been fully edited. Content may change prior to final publication. Citation information: DOI 10.1109/TUFFC.2018.2881358, IEEE Transactions on Ultrasonics, Ferroelectrics, and Frequency Control

III. Results

A. Mesh CFU Results

Figure 6 shows the number of CFUs remaining on the mesh following the ultrasound and sham exposures. The number of meshes that had any CFUs is also given on each bar, so only half of the exposed meshes had any surviving CFUs. The number of CFUs was 1.38±1.68-$\log_{10}$ and 6.80±0.68-$\log_{10}$ for the exposed and sham meshes respectively. Therefore, the average reduction in CFUs in the biofilm by the ultrasound exposure was 5.41-$\log_{10}$.

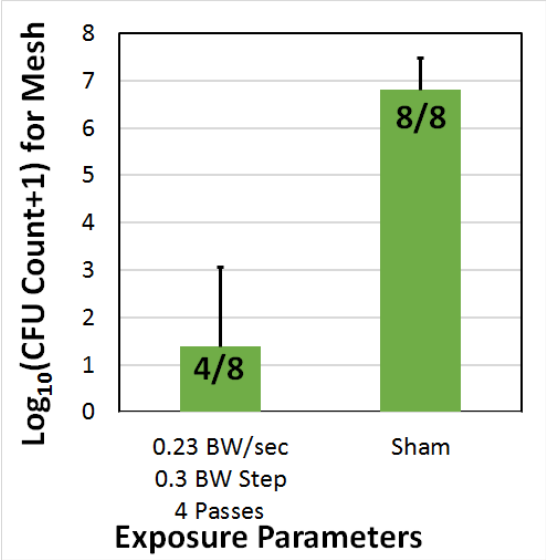

Fig. 6. Count of CFUs surviving on the mesh sample for both the exposed and sham treatments. The error bars correspond to one standard deviation. The numbers on each bar correspond to the number of repetitions for which CFUs were found on the mesh.

B. Results of Mesh Mechanical Properties

In addition to quantifying the number of CFUs surviving on the mesh samples, the impact of the ultrasound exposures on the ultimate tensile strength and maximum strain was also assessed. Figure 7 shows the ultimate tensile force for each of the mesh orientations for the control, sham, and exposed meshes. Similarly, Figure 8 gives the separation between the clamps at the maximum stress for each exposure condition.

We analyzed the data for both the force and the distance using two-way analysis of variance (ANOVA) and the JMP software (Pro 14, the SAS Institute). Both datasets include 90 observations, 15 observations for each combination of orientation (A or B) and exposure level (control, exposed, or sham). Both models include the two factors (orientation and exposure level) and their interactions. The plots of residuals versus predicted values and the normal probability plots of the residuals indicate that the models are adequate. For both the force and the distance, orientation is the only statistically significant effect. In particular, the average force for orientation B is 1.36 N higher than that for orientation A (with a p-value of 0.024), and the average distance for orientation B is 1.33 mm shorter than that for orientation A (with a p-value less than 0.0001).

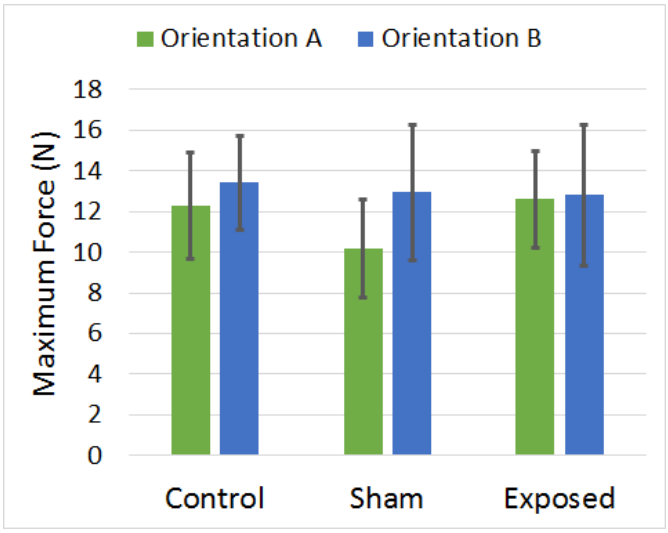

Fig. 7. Ultimate tensile force on mesh for both mesh orientations for the control, sham, and exposed mesh samples. The error bars correspond to one standard deviation.

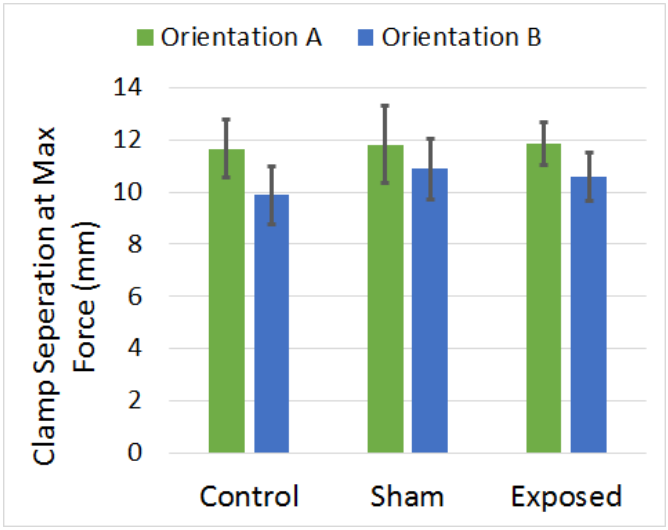

Fig. 8. Clamp separation corresponding to ultimate tensile force on mesh for both mesh orientations for the control, sham, and exposed mesh samples. The error bars correspond to one standard deviation.

IV. Discussion

In this study, the average reduction in CFUs on the mesh following the ultrasound exposures was 5.4-$\log_{10}$ relative to the sham exposures. As a comparison, our average reduction in our earlier studies was 3.8-$\log_{10}$ with a reduction of 4.3-$\log_{10}$ for one of the exposure conditions [10]. The increased biofilm destruction in our present study likely results from several factors. First, when exposing the mesh, the scan speed was slightly slower relative to the beam width than our earlier studies. Previously, we used a 1.1 MHz transducer that at its slowest moved at a speed of 0.4 mm/sec (0.33 beam widths/sec) with a step of 350 µm (0.29 beam widths) between each row. For this study, the 0.9 MHz transducer moved at a speed of 0.3 mm/sec (0.23 beam widths/sec) with a step size of 400 µm (0.3 beam widths). Secondly, the reduction in CFUs was likely biased in our earlier study as most of the exposed mesh samples had no CFUs. Since it is impossible to have a CFU count of less than zero, the maximum average CFU reduction was the

number of CFUs left following the sham exposures or 4.3-$\log_{10}$. Given this limitation from our previous study, the number of bacteria on each mesh was increased for this study by increasing the biofilm growth period from 3 days to 6 days. This increased the number of bacteria on the sham meshes from 4.3-$\log_{10}$ to 6.8-$\log_{10}$. Lastly, operating at a slightly lower frequency might have had an impact; however, our peak rarefactional pressures were also lower in the present study.

Based on our results, the ultrasound exposure had no impact on the mechanical properties of the mesh. The maximum tensile force and corresponding strain were not statistically different between the different exposures. The only statistical difference identified was with respect to mesh orientation. This was not unexpected as the manufacturer of the mesh reported that the ultimate tensile strength of the fabric as well as the percent elongation was different for the different mesh orientations. It was not possible to directly compare our strength and elongation numbers with the manufacturers numbers; however, as the measurements made by the manufacturer were made based on ASTM Standard D-5034 which requires 150 cm^2 of fabric for the test. Our test samples were 1 cm^2. Exposing significantly larger mesh samples to ultrasound was not possible using our mechanically scanned single element transducer due to the scan time required. However, our goal was to conduct a relative comparison of mesh strength between sham, control, and exposed mesh samples. Therefore, increasing the mesh size would have only lengthened the exposure without providing any new information to answer our research question.

V. CONCLUSION

The results of this study continue to confirm the capability of high-intensity ultrasound to destroy bacteria biofilms. The average reduction in CFUs of 5.4-$\log_{10}$ is approaching the FDA definition for high-level disinfectant of 6-$\log_{10}$. Also, this level of biofilm destruction was achieved at lower incident pressures than those used in our earlier *S. aureus* experiments [9, 10], as we chose to operate much closer to the cavitation threshold found in our earlier *E. coli* experiments [11]. Achieving these slightly lower pressure levels *in vivo* will be easier, improving the likelihood of clinical translation. In addition, the ultrasound exposure does not significantly reduce the strength or elastic properties of the mesh. Therefore, it should be possible to treat the bacteria biofilm on the surgical mesh *in vivo* without compromising the structure and function of the mesh in the future.

REFERENCES

[1] M. E. Olson, H. Ceri, D. W. Morck, A. G. Buret, and R. R. Read, "Biofilm bacteria: formation and comparative susceptibility to antibiotics," *Can J Vet Res*, vol. 66, pp. 86-92, 2002.

[2] D. M. Cochrane, M. R. Brown, H. Anwar, P. H. Weller, K. Lam, and J. W. Costerton, "Antibody response to *Pseudomonas aeruginosa* surface protein antigens in a rat model of chronic lung infection," *J Med Microbiol*, vol. 27, pp. 255-261, 1988 1988.

[3] D. De Beer, P. Stoodley, and Z. Lewandowski, "Measurement of local diffusion coefficients in biofilms by microinjection and confocal microscopy," *Biotechnology and Bioengineering*, vol. 53, pp. 151-158, 1997.

[4] J. Rodgers, F. Phillips, and C. Olliff, "The effects of extracellular slime from *Staphylococcus epidermidis* on phagocytic ingestion and killing," *FEMS Immunology and Medical Microbiology*, vol. 9, pp. 109-115, 1994.

[5] C. Vuong, J. M. Voyich, E. R. Fischer, K. R. Braughton, A. R. Whitney, F. R. DeLeo, *et al.*, "Polysaccharide intercellular adhesin (PIA) protects *Staphylococcus epidermidis* against major components of the human innate immune system," *Cellular Microbiology*, vol. 6, pp. 269-275, 2004.

[6] B. W. Trautner and R. O. Darouiche, "Catheter-associated infections: pathogenesis affects prevention," *Arch Intern Med*, vol. 164, pp. 842-850, 2004 2004.

[7] T. A. Bigelow, T. Northagen, T. M. Hill, and F. C. Sailer, "The destruction of *Escherichia coli* biofilms using high-intensity focused ultrasound," *Ultrasound in Medicine & Biology*, vol. 35, pp. 1026-1031, 2009.

[8] J. Xu, T. A. Bigelow, L. J. Halverson, J. M. Middendorf, and B. Rusk, "Minimization of treatment time for in vitro 1.1 MHz destruction of *Pseudomonas aeruginosa* biofilms by high-intensity focused ultrasound," *Ultrasonics*, vol. 52, pp. 668-675, 2012.

[9] T. A. Bigelow, C. L. Thomas, H. Wu, and K. M. F. Itani, "Histotripsy treatment of *S. aureus* biofilms on surgical mesh samples under varying pulse durations," *IEEE Transactions on Ultrasonics, Ferroelectrics, and Frequency Control*, vol. 64, pp. 1420-1428, 2017.

[10] T. A. Bigelow, C. L. Thomas, H. Wu, and K. M. F. Itani, "Histotripsy treatment of *S. Aureus* biofilms on surgical mesh samples under varying scan parameters," *IEEE Transactions on Ultrasonics, Ferroelectrics, and Frequency Control*, vol. 65, pp. 1017-1024, 2018.

[11] G. G. Anderson, J. J. Palermo, J. D. Schilling, R. Roth, J. Heuser, and S. J. Hultgren, "Intracellular bacterial biofilm-like pods in urinary tract infections," *Science*, vol. 301, pp. 105-107, 2003 2003.

[12] W. A. Rutala and D. J. Weber, "Reprocessing endoscopes: United States perspective," *J Hosp Infect*, vol. 56, pp. 27 - 39, 2004.

[13] W. A. Rutala and D. J. Weber, "FDA labeling requirements for disinfection of endoscopes: A counterpoint," *Infection Control and Hospital Epidemiology* vol. 16, pp. 231-235, 1995.

[14] J. C. Carmen, B. L. Roeder, J. L. Nelson, R. L. Robison Ogilvie, R. A. Robison, G. B. Schaalje, *et al.*, "Treatment of biofilm infections on implants with low-frequency ultrasound and antibiotics," *American Journal of Infection Control*, vol. 33, pp. 78-82, 2005.

[15] M. Mavros, S. Athanasiou, V. Alexiou, P. Mitsikostas, G. Peppas, and M. Falagas, "Risk factors for mesh-related infections after hernia repair surgery: A meta-analysis of cohort studies," *World Journal of Surgery*, vol. 35, pp. 2389-2398, 2011.

[16] M. E. Falagas and S. K. Kasiakou, "Mesh-related infections after hernia repair surgery," *Clinical Microbiology and Infection*, vol. 11, pp. 3-8, 2005.

[17] V. M. Sanchez, Y. E. Abi-Haidar, and K. M. F. Itani, "Mesh infection in ventral incisional hernia repair: Incidence, contributing factors, and treatment," *Surgical Infections*, vol. 12, pp. 205-210, 2011.

[18] P. Amid, "Classification of biomaterials and their related complications in abdominal wall hernia surgery," *Hernia*, vol. 1, pp. 15-21, 1997.

[19] T. Lüning and E. J. Spillenaar-Bilgen, "Parastomal hernia: complications of extra-peritoneal onlay mesh placement," *Hernia*, vol. 13, pp. 487-490, 2009.

[20] S. M. Gracewski, H. Miao, and D. Dalecki, "Ultrasonic excitation of a bubble near a rigid or deformable sphere: Implications for ultrasonically induced hemolysis," *The Journal of the Acoustical Society of America*, vol. 117, pp. 1440-1447, 2005.

[21] E. A. Brujan, "The role of cavitation microjets in the therapeutic applications of ultrasound," *Ultrasound in Medicine & Biology*, vol. 30, pp. 381-387, 2004.

[22] S. W. Fong, E. Klaseboer, C. K. Turangan, B. C. Khoo, and K. C. Hung, "Numerical analysis of a gas bubble near bio-materials in an ultrasound field," *Ultrasound in Medicine & Biology*, vol. 32, pp. 925-942, 2006.

[23] K. Y. Chiu, F. T. Cheng, and H. C. Man, "Evolution of surface roughness of some metallic materials in cavitation erosion," *Ultrasonics*, vol. 43, pp. 713-716, 2005.

[24] J. R. Blake and D. C. Gibson, "Cavitation bubbles near boundaries," *Annual Review of Fluid Mechanics*, vol. 19, pp. 99-123, 1987.

[25] A. Pearson, J. R. Blake, and S. R. Otto, "Jets in bubbles," *Journal of Engineering Mathematics*, vol. 48, pp. 391-412, 2004.

[26] M. M. Lima, C. Godoy, P. J. Modenesi, J. C. Avelar-Batista, A. Davison, and A. Matthews, "Coating fracture toughness determined by Vickers indentation: an important parameter in cavitation erosion resistance of WC–Co thermally sprayed coatings," *Surface and Coatings Technology*, vol. 177-178, pp. 489-496, 2004.

[27] S. Hattori and T. Itoh, "Cavitation erosion resistance of plastics," *Wear*, vol. 271, pp. 1103-1108, 2011.

[28] S. H. M. Brown, J. A. Carr, S. R. Ward, and R. L. Lieber, "Passive mechanical properties of rat abdominal wall muscles suggest an important role of the extracellular connective tissue matrix," *Journal of Orthopaedic Research*, vol. 30, pp. 1321-1326, 2012.

[29] I. V. Ogneva, D. V. Lebedev, and B. S. Shenkman, "Transversal stiffness and young's modulus of single fibers from rat soleus muscle probed by atomic force microscopy," *Biophysical Journal*, vol. 98, pp. 418-424, 2010.

[30] F. Dogan and M. S. Celebi, "Quasi-non-linear deformation modeling of a human liver based on artificial and experimental data," *The International Journal of Medical Robotics and Computer Assisted Surgery*, vol. 12, pp. 410-420, 2016.

[31] J. Xu and T. A. Bigelow, "Experimental investigation of the effect of stiffness, exposure time and scan direction on the dimension of ultrasound histotripsy lesions," *Ultrasound in Medicine & Biology*, vol. 37, pp. 1865-1873, 2011.

[32] J. Xu, T. A. Bigelow, G. Davis, A. Avendano, P. Shrotriya, K. Bergler, *et al.*, "Dependence of ablative ability of high-intensity focused ultrasound cavitation-based histotripsy on mechanical properties of agar," *The Journal of the Acoustical Society of America*, vol. 136, pp. 3018-3027, 2014.

[33] J. Xu, T. A. Bigelow, and R. Nagaraju, "Precision control of lesions by high-intensity focused ultrasound cavitation-based histotripsy through varying pulse duration," *IEEE Transactions on Ultrasonics, Ferroelectrics and Frequency Control* vol. 60, pp. 1401-1411, 2013.

[34] E. Vlaisavljevich, Y. Kim, G. Owens, W. Roberts, C. Cain, and Z. Xu, "Effects of tissue mechanical properties on susceptibility to histotripsy-induced tissue damage," *Physics in Medicine and Biology*, vol. 59, pp. 253-270, 2014.

[35] E. Vlaisavljevich, K.-W. Lin, A. Maxwell, M. T. Warnez, L. Mancia, R. Singh, *et al.*, "Effects of ultrasound frequency and tissue stiffness on the histotripsy intrinsic threshold for cavitation," *Ultrasound in Medicine & Biology*, vol. 41, pp. 1651-1667, 2015.

[36] E. Vlaisavljevich, A. Maxwell, M. Warnez, E. Johnsen, C. Cain, and X. Zhen, "Histotripsy-induced cavitation cloud initiation thresholds in tissues of different mechanical properties," *IEEE Transactions on Ultrasonics, Ferroelectrics, and Frequency Control* vol. 61, pp. 341-352, 2014.

[37] Y. Liu, K. A. Wear, and G. R. Harris, "Variation of high-intensity therapeutic ultrasound (HITU) pressure field characterization: Effects of hydrophone choice, nonlinearity, spatial averaging and complex deconvolution," *Ultrasound in Medicine & Biology*, vol. 43, pp. 2329-2342, 2017.

[38] E. G. Radulescu, P. A. Lewin, A. Goldstein, and A. Nowicki, "Hydrophone spatial averaging corrections from 1 to 40 MHz," *IEEE Transactions on Ultrasonics, Ferroelectrics, and Frequency Control*, vol. 48, pp. 1575-1580, 2001.

[39] G. Xing, P. Yang, L. He, and X. Feng, "Spatial averaging effects of hydrophone on field characterization of planar transducer using Fresnel approximation," *Ultrasonics*, vol. 71, pp. 51-58, 2016.

[40] M. S. Canney, M. R. Bailey, and L. A. Crum, "Acoustic characterization of high intensity focused ultrasound fields: A combined measurement and modeling approach," *J. Acoust. Soc. Am.*, vol. 124, pp. 2406-2420, 2008.

[41] O. A. Sapozhnikov, S. A. Tsysar, V. A. Khokhlova, and W. Kreider, "Acoustic holography as a metrological tool for characterizing medical ultrasound sources and fields," *The Journal of the Acoustical Society of America*, vol. 138, pp. 1515-1532, 2015.

[42] P. V. Yuldashev, W. Kreider, O. A. Sapozhnikov, N. Farr, A. Partanen, M. R. Bailey, *et al.*, "Characterization of nonlinear ultrasound fields of 2D therapeutic arrays," *IEEE International Ultrasonics Symposium : [proceedings]. IEEE International Ultrasonics Symposium*, vol. 2012, pp. 1-4, 2012.

[43] B. E. Treeby, J. Jaros, A. P. Rendell, and B. T. Cox, "Modeling nonlinear ultrasound propagation in heterogeneous media with power law absorption using a k-space pseudospectral method," *The Journal of the Acoustical Society of America*, vol. 131, pp. 4324-4336, 2012.

[44] J. Xu, T. A. Bigelow, and G. M. Riesberg, "Impact of preconditioning pulse on lesion formation during high-intensity focused ultrasound histotripsy," *Ultrasound in Medicine & Biology*, vol. 38, pp. 1918-1929, 2012.

[45] J. Xu, T. A. Bigelow, and E. M. Whitley, "Assessment of ultrasound histotripsy–induced damage to *ex vivo* porcine muscle," *Journal of Ultrasound in Medicine*, vol. 32, pp. 69-82, 2013.